



Solar irradiance attenuation by aerosols in cloudless atmosphere: equatorial and temperate examples

Abdelmoula Ben-tayeb^{1,2} · Mohammed Diouri² · Rajae Meziane² · Hanae Steli² · Nadia Yousra Meziani²

Received: 21 May 2020 / Accepted: 31 March 2021 / Published online: 23 April 2021
© Springer Nature Switzerland AG 2021

Abstract

Solar irradiance during daylight hours was calculated using the Iqbal formula, taking into account total and aerosol optical thicknesses extracted from AERONET to determine the attenuation by the atmosphere and by aerosols. Comparison of the results for sites in the equatorial zone (Singapore, San Cristobal and Mbita) and temperate zone (New Delhi, Carthage and Laguna) shows that a cloudless atmosphere weakly reduces solar irradiance in the equatorial zone, which is characterized by more regular meteorology, in comparison to the temperate zone, which is characterized by more human activity. The attenuation in the clear sky (without aerosols) seems to be independent of the region and approximately $8 \pm 1\%$ on average, except for New Delhi, for which maximum attenuation by aerosols (46%) was observed due to the high diversity of seasonal and anthropogenic sources. Attenuation by the atmosphere does not exceed 24% at sites far from industrial pollution sources (Laguna and San Cristobal). For Singapore and Carthage, where anthropogenic aerosol emissions are weak, the attenuation by the atmosphere is around 30%.

Keywords Aerosol optical thickness · Atmospheric attenuation · Size distribution · Solar irradiance · Sun photometer

Introduction

The use of incident solar energy normal to the surface of a given site requires the precise determination of the amount of annual radiation that reaches that site after penetration of the corresponding atmospheric column. The introduction of the total optical thickness of the seasonal cycle in the absence of clouds makes it possible to obtain an accurate estimate of this solar radiation (Ben-tayeb et al. 2020, 2021).

The sun produces the necessary heat and light for all life on Earth. Due to the increasing global demand for energy, it is necessary to study all aspects of the exploitation of solar

radiation (Bai and Wang 1994), in particular the atmosphere and its effects, to determine suitable sites to realize solar farms and avoid and anticipate natural and industrial constraints. The aim of chemistry and material sciences is to develop efficient ways to exploit solar energy and to study the effect of matter on solar radiation through the development of photo-catalysts in solar radiation receptors (Al-Musawi et al. 2018; Touati et al. 2019). Remote sensing is a critical factor in exploiting renewable energies as it enables the study of the components of the atmosphere and to plan, operate and maintain energy infrastructure (Kadhim et al. 2016). Gueymard (1993) developed a model to predict solar radiation at the Earth's surface, but the values are only approximate and there is much uncertainty because each area has its own atmospheric particles, gas molecules, aerosols and clouds. These components are distinct, especially in terms of the concentrations of aerosols which attenuate radiation and affect the climate (Diouri 2018); quantification of the direct effect of aerosols in mega-cities; phenomena of diffusion and absorption of solar radiation (Meziane et al. 2020); and the quantification of the indirect effect of aerosols that modify optical properties of clouds (Steli et al. 2016, 2017). Weather conditions affect the optical properties of aerosols in the atmosphere (Diouri et al. 2009; Tahiri

Responsible Editor: Mohamed Ksibi.

This paper was selected from the 2nd Euro-Mediterranean Conference for Environmental Integration (EMCEI), Tunisia 2019.

✉ Abdelmoula Ben-tayeb
abdelmoulabentayeb@gmail.com

¹ Mechanical Engineering Department, Faculty of Sciences and Technologies, Sultan Moulay Slimane University, Beni-Mellal, Morocco

² Atmospheric Physic Team, Physic Department, Faculty of Science, Mohammed 1St University, Oujda, Morocco

et al. 2016, 2018); for example, frequent dust seasons lead to a predominant contribution of coarse particles, especially in dry periods (Che et al. 2015; Yusuf et al. 2020). Aerosols have been included in atmospheric models since the beginning of this century; this allows a better estimate of the evolution of atmospheric components according to climatic conditions (Diouri 2018; Snoun et al. 2019). The sources of natural and anthropogenic particulate matter in air pollution and the resulting climatic effects have been studied (Hamed et al. 2018). Analysis of the optical properties of aerosols in East Asia has shown that the greatest aerosol loading occurs during the dry season and leads to significant warming of the atmosphere and cooling of the surface, with a reduction caused by humidity after precipitation (Mai et al. 2018). In eastern–northern India, increasing aerosol optical thickness in winter and pre-monsoon seasons leads to high aerosol radiative forcing (Dhar et al. 2017). Aerosol optical studies carried out in the Mediterranean region, which is characterized by different types of aerosols (Esteve et al. 2014; Di Biagio et al. 2018), have confirmed the same trend, with maximum values recorded in summer and minimum values in winter. Natural intensities are greater in southern regions and anthropogenic ones are greater in northern ones (Marsli et al. 2019).

This work is based on optical measurement data obtained from the AERONET network, which constitutes a very important technological development that allows greater competitiveness. These are computational and empirical data associated with parasitic techniques which a fortiori allow faster development (Coccia 2017, 2019, 2020). In this study, we quantify the attenuation of solar radiation by due to aerosol emission for six sites representative of the equatorial and temperate zones. To this end, we integrate the data on the aerosol optical thicknesses (AOT) and total optical thicknesses (TOT) measured by the network AERONET/PHOTONS into the calculation of the attenuated radiation using the PSIX program, based on the Iqbal formula of solar irradiance during the day, taking into account the position of the sun and the latitude. The determination of the particle size distributions (PSDs) and the volume concentrations

allows an appreciation of the linearity between the determined concentrations and the attenuations obtained (Bentayeb et al. 2020).

Methodology

Sample and data

The study periods and characteristics of each study site are given in Table 1. Three sites were chosen as representative of the equatorial zone and three as representative of the temperate zone.

The selected sites are dispersed in their respective zone and can be considered to representative of that zone. They also are located in different regions of the world: the three sites in the equatorial zone (Ecuador, Kenya and Singapore) are very distant from each other and in different climates, as are the three sites in the temperate zone (La Laguna in the the Canary Islands [Atlantic], Carthage in the Mediterranean region and New Delhi in the Indian peninsula). All sites differ in terms of the composition of the atmosphere.

Equatorial zone

San Cristóbal is located on an island near Ecuador in the Pacific Ocean, far from all sources of industrial pollution. Some traces of carbon-rich aerosols were detected, such as smoke and biomass burning aerosols, most likely transported to this region by continental wind currents from Africa, Western Europe and eastern South America (García and Tatiana 2019). The ICIPE (International Centre of Insect Physiology and Ecology) Mbita site is located in Kenya along the shores of Lake Victoria, near one of Kenya's main cities. Mbita is influenced by the lake–land air exchange affected by aerosols caused by traffic and the burning of biomass from neighboring rural areas (Zachary et al. 2018). An analysis by Ngaina et al. (2014) showed that aerosols mainly of dust and sea salt reaching Kenya are transported from the Arab or Indian subcontinent or from the western parts of the

Table 1 Site characteristics and period of the study (AERONET)

Site	Latitude	Longitude	Altitude (m a.s.l.)	Period	
				Start	End
Equatorial zone					
San Cristóbal USFQ (Ecuador)	0.89 S	89.6 W	22	12 January 2019	31 December 2019
ICIP Mbita (Kenya)	0.43 S	34.20 E	1152	1 January 2013	31 December 2013
Singapore (Singapore)	1.29 N	103.78 E	30	1 January 2018	31 December 2018
Temperate zone					
La Laguna (Spain)	28.48 N	16.32 W	568	1 January 2013	31 December 2013
Tunis Carthage (Tunisia)	36.83 N	10.19 E	10	1 January/2019	31 December 2019
New Delhi (India)	28.63 N	77.17 E	240	1 January 2009	31 December 2009

Indian Ocean. Singapore is characterized mostly by aerosol particles in the fine mode, with a small optical thickness, that result from urban pollution (Salinas 2009). Data indicate the presence of particles resulting from the combustion of biomass, with the period July–September coinciding with the typical biomass combustion season (Chew 2013).

Temperate zone

La Laguna is characterized primarily by marine aerosols, with the maximum AOT recorded in June–August due to the mixture of dust and sea salt transport (Rodríguez et al. 2011, 2012). Analysis of the dust episodes in North Africa indicate that mineral dust is the main contributor to the dominance of the aerosol coarse mode. In Carthage (Tunisia), secondary aerosols are produced during the summer by atmospheric photochemistry (Saad et al. 2016). The megalopolis New Delhi very polluted and heavily populated. It is characterized by the seasonal variability of AOT, with the maximum observed in June and November and the minimum in March and September. The highest AOT is observed after the monsoon and is attributed to the significant contribution of urban aerosol and biomass combustion. During the pre-monsoon season, most mixed types of dust and aerosols dominate. The maximum AOT at short wavelengths is observed in June and November, and the maximum AOT at long wavelengths appears in June (Tiwari 2016). Between April and June, desert aerosols dominate with 1.17 ± 0.65 of AOT at $0.5\text{-}\mu\text{m}$ diameter (Sachchidanand et al. 2005).

Measures used

The spectral total optical thickness at $0.5\ \mu\text{m}$ ($TOT_{0.5}$) is the sum of the contributions of Rayleigh interactions, aerosols and gas, given by AERONET. The value generally varies, with the monthly mean ranging from 0.1 to 0.6 except for New Delhi, where the average value is 0.8 (Fig. 1).

The equatorial sites are characterized by a relative constant and regular seasonal $TOT_{0.5}$ of around 0.6 for ICIP Mbita, 0.4 for Singapore and 0.3 for San Cristóbal. In contrast, the three sites in the temperate zone are more variable, with the lowest $TOT_{0.5}$ of 0.2 at La Laguna, a site located far from pollution sources, and the highest (> 0.6) always at New Delhi due to the high abundance of both natural and anthropogenic aerosols; the $TOT_{0.5}$ is 0.4 at Carthage where there are few human activities.

Data analysis procedure

Most observation networks of climate use the sun photometer as a monitoring device; in this context, AERONET provides a wide range of parameters from daily measurements,

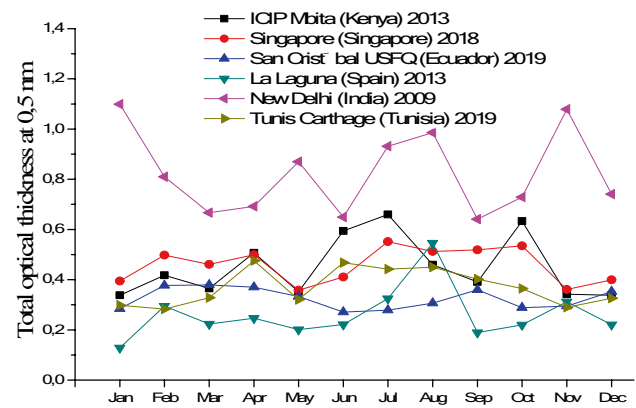


Fig. 1 Monthly variation of total optical thickness at $0.5\ \text{nm}$ ($TOT_{0.5\ \mu\text{m}}$)

including the optical thicknesses of all components of the atmosphere, volume particle size distributions, spectral refractive index and single scattering albedo (Holben et al. 2006). Based on an analysis of AERONET data collected in Eastern Europe, natural factors were found not to have a significant effect on temporal variations in the optical thickness of aerosols in mega cities, such as Moscow (Chubarova et al. 2016). In the West African region, a study of the properties associated with the absorption and size distribution of aerosols identified the four sources of aerosols: desert dust, biomass burning aerosols, urban aerosols and gas flaring (Fawole et al. 2016). These parameters were determined from almucantar and direct solar measurements. The uncertainties of AOT and TOT vary according to the wavelength of the solar radiation (Holben et al. 1999; Eck et al. 1999).

In this study, the monthly average AOT was stable during the study year for ICIP-Mbita at around 0.2 at the wavelength $0.5\ \mu\text{m}$, except for in the dry season (June–August) when there was a small increase and it did not reach 0.5 (Fig. 2). Due to the distant sources of pollution at San Cristóbal, low AOT was registered at this site during the study year, with the monthly average AOT just above 0.2 during the period of February–April and September. In Singapore, the AOT remained almost stable during the study year except for two periods of February–April and July–October when there was a slight increase. In New Delhi, the diversity of major aerosol sources implied extreme changes and high values throughout the study year, with maximum values in November and January. La Laguna seemed to be relatively clean site because it is located far from all sources of pollution, but it is influenced by desert aerosols advectations from the Sahara, which reach a maximum in August. In Carthage, the AOT increased from the beginning of spring to the end of the summer, with a decrease to 0.16 at $0.5\ \mu\text{m}$ in the precipitation period; the maximum of $AOT_{0.5}$ reached 0.32 in April.

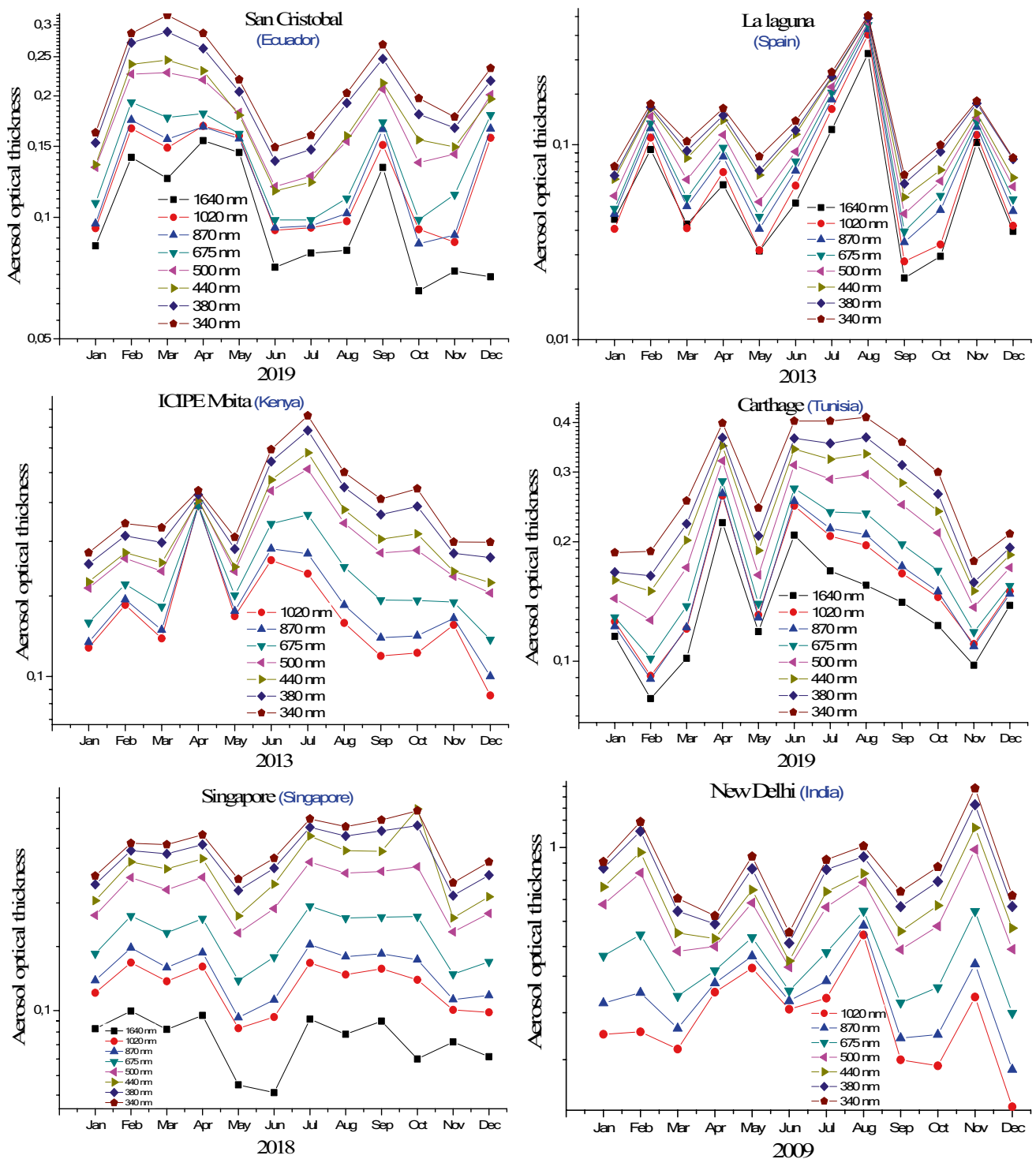


Fig. 2 Monthly average of aerosol optical thickness at study sites in the equatorial zone (left) and in temperate zone (right)

The size of particles is one of the most important criteria to characterize the behavior of aerosols. The particle size distribution can be determined from many inversion

algorithms (Diouri and Sanda 1997; Diouri et al. 1997) using data of AOT. Based on previous studies, Dubovik et al. (2000) modeled particle volume size distribution by the bimodal lognormal as given in Eq. 1:

$$\frac{dV}{d \ln r} = \frac{V_f}{\sqrt{2\pi} \ln \sigma_f} \exp\left(-\frac{|\ln r - \ln r_f|^2}{2(\ln \sigma_f)^2}\right) + \frac{V_c}{\sqrt{2\pi} \ln \sigma_c} \exp\left(-\frac{|\ln r - \ln r_c|^2}{2(\ln \sigma_c)^2}\right) \quad (1)$$

where r_f and r_c are respectively fine and coarse mode median radius and V_f and V_c are their respective amplitudes, as represented in Table 2. We represent the total volumetric concentration of the particles by $V_t \cdot \sigma_c$ and σ_f , which are coarse and fine mode standard deviation, respectively.

AERONet allows the volume PSDs to be determined. Here, we present the monthly average volume PDDs at all six study sites (Fig. 3). The bimodality variation of the distribution at all sample sites should be noted. The peak is for particles in the fine mode, between 0.04 and 1 μm ; the second peak is for particles in the coarse mode, between 1 and 10 μm .

The concentrations vary from site to site depending on the aerosol sources. At ICIPE Mbita, a maximum of coarse particles with a mean radius of around 2.55 μm (Table 2) occur as a result of mineral dust throughout the year and especially during the summer. Very low concentrations of the two modes of particles are recorded at San Cristóbal, with a small increase in the volume concentration of coarse particles in February, reaching 0.04 $\mu\text{m}^3/\mu\text{m}^2$ (corresponding to a mean radius of 5 μm). The average concentrations of fine and coarse particles seem to be equal in Singapore (Table 2). In La Laguna, very low average concentrations of fine particles are found; in contrast, notable concentrations of coarse particles (0.22 $\mu\text{m}^3/\mu\text{m}^2$) relative to the mean radius of 2.2 μm are observed in August. In New Delhi, the large concentration of fine particles recorded in November and January coincide with large biomass combustions; for coarse particles, the maximum concentrations are observed in the April–August period, reaching 0.25 $\mu\text{m}^3/\mu\text{m}^2$ (corresponding to a mean radius of 4 μm) in April. At Carthage, there is a predominance of coarse particles in the dry season (June–August), with the maximum concentration reaching

0.074 $\mu\text{m}^3/\mu\text{m}^2$ in June (corresponding to a mean radius of 1.7 μm).

Solar irradiance on the Earth's surface is related to the geographical latitude (φ), the eccentricity factor of the earth's orbit (E_0), the solar declination (δ), the solar constant (I_{sc}) and the hour angle of the sunrise (ω_s) (Iqbal 1983). The extraterrestrial irradiance on a horizontal surface during the day from sunrise to sunset is given by Eq. (2):

$$I_0 = (24/\pi) I_{sc} E_0 \cos \varphi \cos \delta [\sin \omega_s - \omega_s \cos \omega_s] \quad (2)$$

Due to aerosol extinction, molecular scattering (or Rayleigh) and gas absorption, solar irradiance is attenuated. This attenuation may be expressed with the Bouguer law by Eq. (3):

$$I(\lambda) = I_0(\lambda) \cdot \exp[-m_{\text{air}} \cdot \text{TOT}(\lambda)] \quad (3)$$

where m_{air} is the relative air mass expressed by Kasten et al. (1989).

To determine the monthly attenuations of solar irradiance by the atmosphere and by the aerosols, we calculated the solar irradiance at the top of atmosphere I_0 and inserted TOT and AOT values through the PSIX program, obtaining the atmospheric attenuation (TE) and aerosol attenuation (AE), respectively, as shown in Fig. 4.

Results and discussion

The results show that solar energy generation decreases with deterioration of the air quality and that compared to other atmospheric parameters, the rate of solar irradiance attenuation due to aerosols is the dominant factor driving

Table 2 Annual mean particle size distribution parameters: fine and coarse median radius, fine and coarse volume concentrations and total volume concentration

Site	Fine mode		Coarse mode		V_t ($\mu\text{m}^3/\mu\text{m}^2$)
	r_f (μm)	V_f ($\mu\text{m}^3/\mu\text{m}^2$)	r_c (μm)	V_c ($\mu\text{m}^3/\mu\text{m}^2$)	
Equatorial zone					
San Cristóbal USFQ (Ecuador)	0.16	0.014	2.68	0.039	0.053
ICIP Mbita (Kenya)	0.16	0.026	2.55	0.102	0.128
Singapore (Singapore)	0.19	0.046	2.76	0.059	0.105
Temperate zone					
La Laguna (Spain)	0.16	0.010	2.13	0.061	0.071
Tunis Carthage (Tunisia)	0.14	0.020	2.62	0.080	0.100
New Delhi (India)	0.15	0.060	2.83	0.292	0.352

r_f , r_c , Fine and coarse median radius, respectively; V_f and V_c , fine and coarse volume concentrations, respectively; V_t total volume concentration

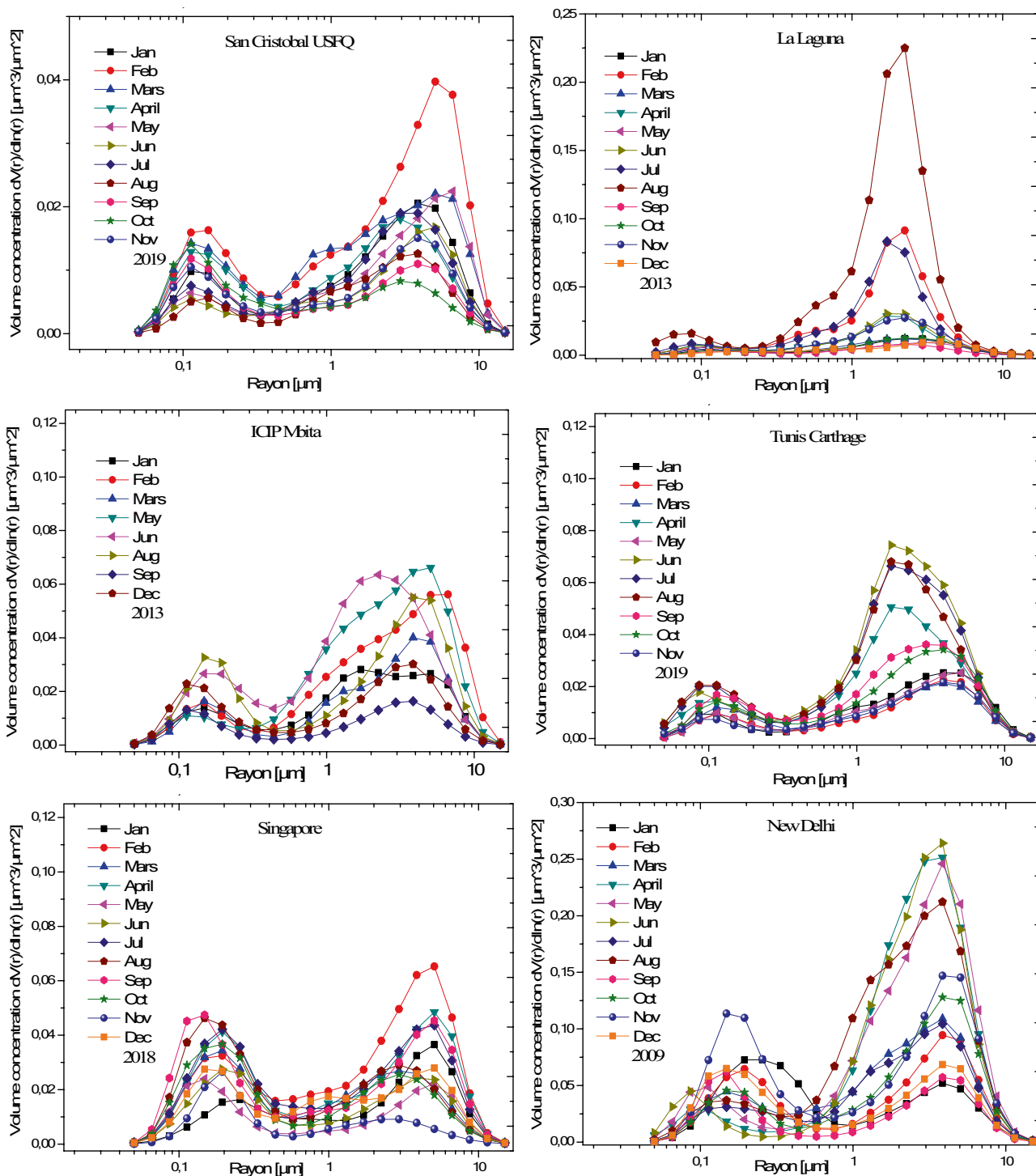


Fig. 3 Monthly average volume particle size distributions at study sites in the equatorial zone (left) and in temperate zone (right)

this deterioration (Yu et al. 2020). A study in which a prediction model of solar radiation in a clear sky was based on four climate parameters (ozone, water vapor, nitrogen dioxide and the Ångström turbidity) showed that air pollution with aerosols can lead to a loss of > 20% of the collectible solar

energy (Calinoiu et al. 2013). The Global Climate Model (Bergen et al. 2017) shows that aerosol particles reduce solar energy by 15–25% in Singapore during agricultural burn events and by more than 25% in the Arabian Peninsula due to dust, and that in China anthropogenic particles in polluted

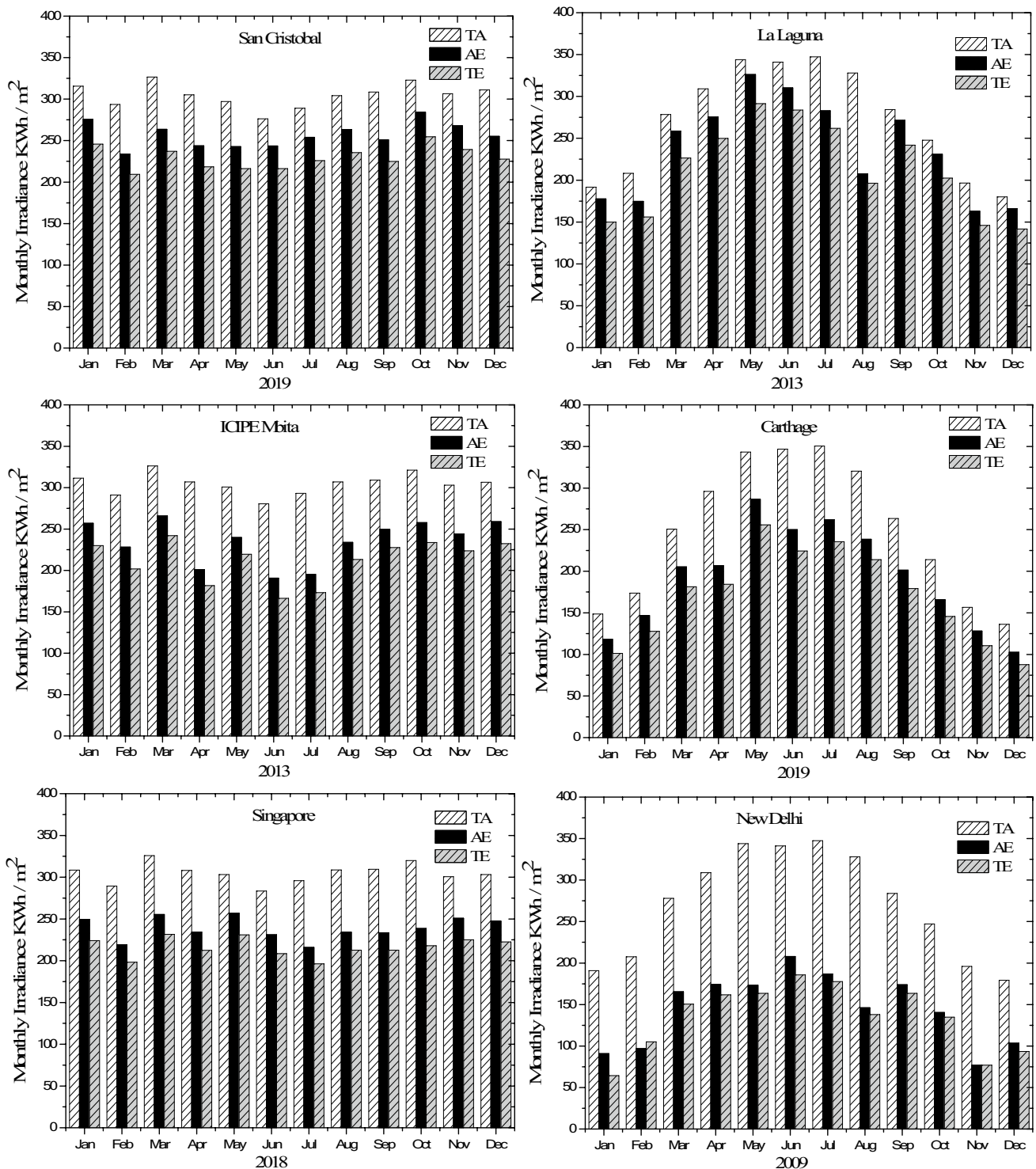


Fig. 4 Monthly solar irradiance at the top of the atmosphere (*TA*), with aerosol extinction (*AE*), and with total extinction (*TE*) at study sites in the equatorial zone (left) and in temperate zone (right)

areas contribute to a decrease of 17% of the solar irradiance. A study targeting the New Delhi site noted that aerosols reduce solar radiation by 40% (Millstein and Fischer 2014).

The annual *TE* and *AE* attenuation rates (Table 3) are highest when the attenuation by aerosols is large, thereby confirming the attenuation dominance of aerosols over other components of the atmosphere.

Table 3 Annual average of attenuation of solar irradiance by atmosphere and by aerosols

	Total extinction (%)	Aerosol extinction (%)
Equatorial zone		
San Cristóbal USFQ (Ecuador)	24.77	15.78
ICIP Mbita (Kenya)	30.39	22.8
Singapore (Singapore)	29.08	21.59
Temperate zone		
La Laguna (Spain)	21.76	12.63
Tunis Carthage (Tunisia)	31.75	22.93
New Delhi (India)	50.33	46.58

At the equator, the incident solar irradiance at the top of the atmosphere (I_0) is relatively the same every day of the year. The monthly attenuation of solar irradiance by the atmosphere and by aerosols in Singapore and their deviations remain almost constant. For ICIP Mbita, the attenuation of the solar irradiance is high during April, June and July, corresponding to the appearance of the desert aerosol. Small monthly attenuation rates of solar irradiance are recorded at San Cristóbal. The maximum attenuation of the solar irradiance by the atmosphere in Carthage, 38%, is recorded in April. For La Laguna, the maximum attenuation is recorded in August and July. The influence of the combination of desert and urban aerosols attributed to human activity and biomass combustion emissions at New Delhi lead to a very strong atmospheric attenuation of the solar irradiance. Finally, the temperate sites (Fig. 4, right side) show seasonal attenuation irregularities, with an increase in the spring and summer, which is most notable as a steep increase in New Delhi, and flat-shaped histograms relative to equatorial sites (Fig. 4, left side) where monthly attenuation of the solar irradiance seems more regular and low.

Conclusions

Solar irradiance depends on constant geographic factors, such as altitude, latitude and season, and on variable factors, such as atmospheric load, presence of clouds and aerosols; the latter are considered to be the most important factors influencing the attenuation solar irradiance. The inclusion of TOT and AOT data from six AERONET sites (three in the equatorial zone and three in the northern temperate zone) in the PSIX calculation program allows the attenuation of solar irradiance by aerosols and by the atmosphere to be quantified. The difference between the two zones lies in the altitude of the atmosphere, which is greatest in the equator, and in the length of the day, which is regular all year round in the equatorial zone, while it lengthens in summer and

shortens in winter in the temperate zone. The most significant difference observed is related to the effect of pollution and desert aerosols.

Monthly average of the volume particle size distribution shows low concentrations for both fine and coarse modes throughout the year for the equatorial zone. For the temperate zone, La Laguna and Carthage register a noticeable rise in the concentration of particles of the coarse mode during the summer due to the influence of the desert mineral dust advections, while there is a very low concentration of particles of the fine mode. In New Delhi, high concentrations of particles of both modes, but especially those of the coarse mode, are found from April to August. The large increases in AOT observed depend on seasonal phenomena of aerosol production from desert storms and biomass combustion. The solar irradiance attenuation by the total atmosphere is directly linked to aerosol volume concentration, as reported earlier by Ben-tayeb et al. (2020).

The monthly solar irradiance in the equatorial zone is almost constant, while in the temperate zone, the atmospheric attenuation is stronger in the summer and autumn or spring depending on the appearance of desert aerosol advections. The highest attenuation—around the order of 50%—was recorded in Delhi where the desert aerosol combines with the urban one attributed to human activity and aerosols emitted by biomass combustions. The results of direct attenuation of solar irradiance by aerosols are comparable to those determined by other models and techniques. The study of the attenuation of solar irradiance by atmospheric components presents a degree of uncertainty due to the changing nature of the atmosphere.

The results of this study can be generalized to specific areas of the Earth that have the same optical properties of aerosols as well as the same source of aerosols, taking into account that while other cloudless atmospheric components (molecules and water vapor) affect the attenuation of solar irradiance relatively less than aerosols, they do so at almost a constant level. For example, in the North African region, the mean attenuation of solar irradiance by aerosols is of the order of 22% due to nearly identical air quality conditions dominated by desert aerosols transported by seasonal air masses coming from the Sahara. This value can be generalized to the rest of North Africa's sites in the southern Mediterranean. It is necessary to study the optical properties of aerosols for each site.

This study is the start of a comprehensive study of the effect of atmospheric components on solar radiation, including the effect of clouds, the study of which remains a challenge in this field.

Acknowledgments The authors want to thank AERONET's IPs: Maria del Carmen Cazorla, Emilio Cuevas-Agullo, Philippe Goloub, Francisco Javier Expósito Gonzalez, Brent Holben and Soo-Chin Liew.

Funding Not applicable.

Declarations

Conflict of interest The authors declare that they have no conflict of interest.

References

- Al-Musawi OAH, Khadom AA, Ahmadun FB, Biak DR (2018) Water distillation in a combined solar still and solar pond system: Iraq as a case study. *Euro-Mediterr J Environ Integr*. <https://doi.org/10.1007/s41207-018-0057-x>
- Bai J, Wang G (1994) The analysis for the primary factors affecting the solar global radiation. *Plateau Meteorol* 13(4):103–106
- Ben-tayeb A, Diouri M, Meziane R, Steli H (2020) Solar radiation attenuation by aerosol: application to solar farms. *Air Qual Atmos Health* 13:259–269. <https://doi.org/10.1007/s11869-020-00790-1>
- Ben-tayeb A, Diouri M, Tahiri A, Meziane R (2021) Optical properties and effects on direct solar irradiance of aerosols: Asian East case. *E3S Web Conf* 234:00054. <https://doi.org/10.1051/e3sconf/202123400054>
- Bergin MH, Ghoroi C, Dixit D, et al (2017) Large reductions in solar energy production due to dust and particulate air pollution. *Environ Sci Technol Lett* 4(8):339–344. <https://doi.org/10.1021/acs.estlett.7b00197>
- Calinoiu D, Paulescu M, Ionel I, et al (2013) Influence of aerosols pollution on the amount of collectable solar energy. *Energy Convers Manag* 70:76–82. <https://doi.org/10.1016/j.enconman.2013.02.012>
- Che H, Zhao H, Wu Y, et al (2015) Analyses of aerosol optical properties and direct radiative forcing over urban and industrial regions in Northeast China. *Meteorol Atmos Phys* 127:345–354. <https://doi.org/10.1007/s00703-015-0367-3>
- Chew BN, Campbell JR, Salinas SV, et al (2013) Aerosol particle vertical distributions and optical properties over Singapore. *Atmos Environ* 79:599–613. <https://doi.org/10.1016/j.atmosenv.2013.06.026>
- Chubarova NY, Poliukhov AA, Gorlova ID (2016) Long-term variability of aerosol optical thickness in Eastern Europe over 2001–2014 according to the measurements at the Moscow MSU MO AERONET site with additional cloud and NO₂ correction. *Atmos Meas Tech* 9(2):313–334. <https://doi.org/10.5194/amt-9-313-2016>
- Coccia M (2017) Sources of technological innovation: radical and incremental innovation problem-driven to support competitive advantage of firms. *Technol Anal Strateg Manag* 29(9):1048–1061. <https://doi.org/10.1080/09537325.2016.1268682>
- Coccia M (2019) A Theory of classification and evolution of technologies within a Generalized Darwinism. *Technol Anal Strateg Manag* 31(5):517–531. <https://doi.org/10.1080/09537325.2018.1523385>
- Coccia M, Watts J (2020) A theory of the evolution of technology: technological parasitism and the implications for innovation management. *J Eng Technol Manag* 55:101552. <https://doi.org/10.1016/j.jengtman.2019.11.003>
- Dhar P, De BK, Banik T, Gogoi MM, Babu SS, Guha A (2017) Atmospheric aerosol radiative forcing over a semi-continental location Tripura in North-East India: model results and ground observations. *Sci Total Environ* 580:499–508
- Di Biagio C, Di Sarra A, Meloni D, Monteleone F, Piacentino S, Sferlazzo D (2009) Measurements of Mediterranean aerosol radiative forcing and influence of the single scattering albedo. *J Geophys Res Atmos* 114(6):D06211. <https://doi.org/10.1029/2008JD011037>
- Diouri M (2018) *Atmosphère et climat*, volume 1. Université Mohamed Premier, Oujda
- Diouri M, Sanda IS (1997) Deduction of particle size distribution from aerosol optical depth CLEOPATRE I code. *J Aerosol Sci* 28:459
- Diouri M, El Hitmy M, Sanda IS, Jaenicke R, Kulzer S, Leiterer U, Schutz L, Schultz KH (1997) Indirect determination of particle size distribution using a sunphotometer at Lidenberg (Germany) and Oujda (Morocco). *J Aerosol Sci* 28:401
- Diouri M, Hoyningen-Huene WV, Zarrouk T, Dinter T, Kokhanovsky A, Burrows JP (2009) Determination of aerosol particle size distribution for mineral dust during the SAMUM campaign. In: *European Aerosol Conference*, 6–11 September 2009, Karlsruhe. Abstract T052A16
- Dubovik O, Smirnov A, Holben BN, et al (2000) Accuracy assessments of aerosol optical properties retrieved from Aerosol Robotic Network (AERONET) Sun and sky radiance measurements. *J Geophys Res Atmos* 105(D8):9791–9806. <https://doi.org/10.1029/2000JD900040>
- Eck TF, Holben BN, Reid JS, et al (1999) Wavelength dependence of the optical depth of biomass burning, urban, and desert dust aerosols. *J Geophys Res* 104(D24):31333–31349. <https://doi.org/10.1029/1999JD900923>
- Esteve AR, Estellés V, Utrillas MP, Martínez-Lozano JA (2014) Analysis of the aerosol radiative forcing over a Mediterranean urban coastal site. *Atmos Res* 137:195–204. <https://doi.org/10.1016/j.atmosres.2013.10.009>
- Fawole OG, Cai X, Levine JG, Pinker RT, MacKenzie AR (2016) Detection of a gas flaring signature in the AERONET optical properties of aerosols at a tropical station in West Africa. *J Geophys Res* 121(24):14513–14524. <https://doi.org/10.1002/2016JD025584>
- García M, Tatiana S (2019) Caracterización del aerosol troposférico en la zona urbana del Valle de Aburrá, a partir de mediciones satelitales e in-situ E. Tecnológico de Antioquia. <https://dspace.tdea.edu.co/handle/tda/489>. Accessed 10 Dec 2019
- Gueymard C (1993) Critical analysis and performance assessment of clear sky solar irradiance models using theoretical and measured data. *Sol Energy* 51(2):121–138
- Hamed Y, Hadji R, Redhaounia B, Zighmi K, Bâali F, El Gayar A (2018) Climate impact on surface and groundwater in North Africa: a global synthesis of findings and recommendations. *Euro-Mediterr J Environ Integr* 3:25. <https://doi.org/10.1007/s41207-018-0067-8>
- Holben BN, Tanré D, Smirnov A, et al (1999) Optical properties of aerosol from long term ground-based AERONET measurements. In: *Proc. ALPS99*, 17–23 January 1999, Meribel. WK1-O-19. https://scholar.google.com/scholar_lookup?title=Optical%20properties%20of%20aerosols%20from%20long%20term%20groundbased%20aeronet%20measurements&publication_year=1999&author=Holben%20BN&author=Tanre%20D&author=Smirnov%20A&author=Eck%20TF&author=Slutsker%20I&author=Dubovik%20O&author=Lavenu%20C&author=Abuhassen%20CN&author=Chatenet%20CB
- Holben BN, Eck TF, Slutsker I, et al (2006) Aeronet's Version 2.0 quality assurance criteria. In: *SPIE Asia-Pacific Remote Sensing. Proceedings Remote Sensing of the Atmosphere and Clouds*, 8 December 2006, Goa. 6804:64080Q. <https://doi.org/10.1117/12.706524>
- Iqbal M (1983) *An introduction to solar radiation*. Academic Press, Toronto
- Kadhim N, Mourshed M, Bray M (2016) Advances in remote sensing applications for urban sustainability. *Euro-Mediterr J Environ Integr*. <https://doi.org/10.1007/s41207-016-0007-4>
- Kasten F, Young AT (1989) Revised optical air mass and approximation formula. *Appl Opt* 28:4735–4738

- Mai B, Deng X, Li Z et al (2018) Aerosol optical properties and radiative impacts in the Pearl River Delta region of China during the dry season. *Adv Atmos Sci* 35(2):195–208. <https://doi.org/10.1007/s00376-017-7092-4>
- Marsli I, Diouri M, Comparison of aerosol radiative forcing in dry and humid Subtropical area, poster participation in European Aerosol Conference - EAC 2019, Gothenburg, Sweden, 25–30 Aug 2019
- Meziane R, Diouri M, Ben-tayeb A (2020) Optical aerosol properties of megacities: inland and coastal cities comparison. *Air Qual Atmos Health* 13:25–33. <https://doi.org/10.1007/s11869-019-00769-7>
- Millstein DE, Fischer ML (2014) Reflective ‘cool’ roofs under aerosol-burdened skies: radiative benefits across selected Indian cities. *Environ Res Lett* 9(10):104014. <https://doi.org/10.1088/1748-9326/9/10/104014>
- Ngaina JN, Mutai BK, Ininda JM, Muthama JN (2014) Monitoring spatial-temporal variability of aerosol over Kenya. *Ethiop J Environ Stud Manag* 7(3):244–252. <https://doi.org/10.4314/ejesm.v7i3.3>
- Rodríguez S, Alastuey A, Alonso-Pérez S, et al (2011) Transport of desert dust mixed with North African industrial pollutants in the subtropical Saharan Air Layer. *Atmos Chem Phys* 11:6663–6685. <https://doi.org/10.5194/acp11-6663-2011>
- Rodríguez E, Toledano C, Cachorro V, et al (2012) Comparison of aerosol optical properties at the sub-arctic stations ALOMAR-Andenes, Abisko and Sodankylä in late spring and summer 2007. *Atmos Res* 107:20–30. <https://doi.org/10.1016/j.atmosres.2011.12.003>
- Saad M, Trabelsi A, Masmoudi M, Alfaro SC (2016) Spatial and temporal variability of the atmospheric turbidity in Tunisia. *J Atmos Solar Terr Phys* 149:93–99. <https://doi.org/10.1016/j.jastp.2016.10.001>
- Sachchidanand S, Shambhu N, Ramesh K, Risal S (2005) Aerosols over Delhi during pre-monsoon months: characteristics and effects on surface radiation forcing. *Geophys Res Lett* 32:L13808. <https://doi.org/10.1029/2005GL023062,2005>
- Salinas SV, Chew BN, Liew SC (2009) Retrievals of aerosol optical depth and Ångström exponent from ground-based Sun-photometer data of Singapore. *Appl Opt* 48(8):1473–1484. <https://doi.org/10.1364/AO.48.001473>
- Snoun H, Kanfoudi H, Bellakhal G, Chahed J (2019) Validation and sensitivity analysis of the WRF mesoscale model PBL schemes over Tunisia using dynamical downscaling approach. *Euro-Mediterr J Environ Integr* 4:13. <https://doi.org/10.1007/s41207-019-0103-3>
- Steli H, Marsli I, Diouri M, Tahiri A (2016) Aerosol and cloud optical depths (AOD and COD) in the equatorial area. *Environ Sci Hikari Ltd* 4(1):39–51. <https://doi.org/10.12988/es.2016.51217>
- Steli H, Diouri M, Marsli I, Meziane R (2017) Aerosol PSD and occurrence frequencies of clouds in the equatorial area. *JMES* 8(2):648–656
- Tahiri A, Diouri M, Steli H, Marsli I, Meziane R, Ben-tayeb A (2016) Desert aerosol optical properties in Morocco. *Environ Sci Hikari Ltd* 4:63–78. <https://doi.org/10.12988/es.2016.631>
- Tahiri A, Diouri M, Barkani J (2018) Optical properties of desert aerosol-I. *J Mater Environ Sci* 9(10):2870–2883
- Tiwari S, Tiwari S, Hopke PK et al (2016) Variability in optical properties of atmospheric aerosols and their frequency distribution over a mega city “New Delhi.” *India Environ Sci Pollut Res* 23:8781. <https://doi.org/10.1007/s11356-016-6060-3>
- Touati A, Lobna J, Wahiba N, Sayadi S (2019) Photocatalytic degradation of sulfur black dye over Ce-TiO₂ under UV irradiation: removal efficiency and identification of degraded species. *Euro-Mediterr J Environ Integr* 4(1):1–16. <https://doi.org/10.1007/s41207-018-0086-5>
- Yu L, Zhang M, Wang L, Lu Y, Li J (2020) Effects of aerosols and water vapour on spatial-temporal variations of the clear-sky surface solar radiation in China. *Atmos Res* 248:105162. <https://doi.org/10.1016/j.atmosres.2020.105162>
- Yusuf N, Tilmes S, Gbobaniyi E (2020) Multi-year analysis of aerosol optical properties at various timescales using AERONET data in tropical West Africa. *J Aerosol Sci* 151:105625. <https://doi.org/10.1016/j.jaerosci.2020.105625>
- Zachary M, Niu SJ, Lü JJ (2018) Aerosol optical and micro-physical characteristic derived from AERONET in Kenya. *Open Access Library J* 5:e4551. <https://doi.org/10.4236/oalib.1104551>